Chinese Journal of
POLYMER SCIENCE

RESEARCH ARTICLE

https://doi.org/10.1007/s10118-026-3677-7
Chinese J. Polym. Sci. **2026**, *44*, 3053–3065

On-demand Peelable UV-curable Adhesives with Superior Bonding Strength: Rational Molecular Engineering of Cohesion-adhesion Synergy

Wen-Qian Liu[a], Peng Wang[b], Hao-Kai Yuan[a], Lin Zhang[a], Bin Chen[a], Hong-Fei Jiang[a], Yi-Ran Wang[a], Lu Wang[a], Shu-Sheng Li[a], and Chuan-Yong Zong[a,c*]

[a] *School of Chemistry and Chemical Engineering, Shandong Provincial Key Laboratory of Extreme Environment-tolerant Specialty Chemicals, University of Jinan, Jinan 250022, China*
[b] *Shandong Institute of Non-Metallic Materials, Jinan 250031, China*
[c] *School of Materials Science and Engineering, Tianjin University, Tianjin 300072, China*

Electronic Supplementary Information

Abstract On-demand peelable adhesives represent a pivotal green chemistry research avenue; however, they confront a critical challenge in reconciling robust interfacial bonding strength with efficient peelability. Herein, a cohesion-adhesion synergy-guided molecular engineering strategy was developed to fabricate UV-curable adhesives with the integrated properties of superior bonding strength and hot water-triggered peelability. The adhesive was formulated with custom-synthesized difunctional polyurethane acrylate (PM1) as the crosslinker, which was blended with complementary acrylate monomers. PM1 constructed a robust yet adaptable crosslinking network to ensure high cohesive strength; its polytetrahydrofuran diol- and polyester diol-derived soft segments endowed the network with superior molecular chain mobility and stress dissipation capacity. Additionally, the incorporation and compositional optimization of polar acrylate monomers modulate the cohesive energy, surface wettability, and interfacial adhesion of the substrate, thus realizing synergistic enhancement of the cohesive and adhesive properties. Systematic experimental investigations and molecular dynamics simulations were conducted to determine the structure-property relationships governing the composition, bonding performance, and mechanical properties of UV-curable adhesives. The optimized formulation achieved high shear strength (>5 MPa, glass substrates), excellent mechanical properties (tensile strength: 12.80 MPa, elongation at break: 313.70%), and good thermal stability (5 wt% weight-loss temperature > 240 °C). Notably, the developed adhesives realize rapid, complete, and residue-free debonding within 3 min of immersion in 60 °C water, where hydration-induced disruption of adhesive-substrate contact attenuates interfacial interactions. Additionally, the peeled adhesive can be recycled repeatedly after drying while retaining its excellent interfacial bonding performance. This study provides a versatile and scalable strategy for the rational design of high-performance functional adhesives, thereby paving the way for recycling electronic products and sustainable manufacturing.

Keywords Peelable adhesives; Polyurethane acrylate; Cohesion-adhesion synergy; Recyclable; Molecular dynamics simulations

Citation: Liu, W. Q.; Wang, P.; Yuan, H. K.; Zhang, L.; Chen, B.; Jiang, H. F.; Wang, Y. R.; Wang, L.; Li, S. S.; Zong, C. Y. On-demand peelable UV-curable adhesives with superior bonding strength: rational molecular engineering of cohesion-adhesion synergy. *Chinese J. Polym. Sci.* **2026**, *44*, 3053–3065.

INTRODUCTION

High-performance adhesives are pivotal functional materials in advanced manufacturing processes and play indispensable roles in electronics, automotive engineering, chip packaging, aerospace, and other high-value sectors.[1–4] Among them, UV-curable acrylate adhesives have become a research hotspot in the adhesive field over the past decade because of their fast curing speed, excellent mechanical properties, and wide range of applicable substrates, which can meet the current demand for high efficiency and low energy consumption.[5,6] However, traditional UV-curable acrylate adhesives construct robust three-dimensional cross-linked networks upon curing, rendering the bonded components intractable to disassembly, recycling, and repair. This limitation is particularly prominent in scenarios such as electronic waste recycling and temporary bonding and has become a core bottleneck restricting the sustainable development of the industry. Therefore, the rational design and scalable fabrication of peelable UV-curable acrylate adhesives has emerged as a critical challenge that demands immediate attention.

Various synthetic and functional modification strategies have been explored for the development of advanced adhesives with on-demand debonding capabilities. For instance,

* Corresponding author, E-mail: chm_zongcy@ujn.edu.cn
Received February 6, 2026; Accepted March 18, 2026; Published online June 8, 2026

stimulus-responsive structural units are integrated into the polymer matrix, enabling reversible dissociation/recombination of the polymer network upon exposure to external triggers, including heat,[7–13] light,[14–17] magnetic fields,[18–21] and electrical stimuli.[22–24] However, the intricate physicochemical characteristics of adhesive systems render the achievement of consistently reliable and precisely tunable adhesion a formidable challenge. Compared to the strategy of incorporating stimuli-responsive moieties into the adhesive network to achieve stimuli-triggered regulation of network structures, anchoring and regulating the interfacial adhesion behavior represents a more ingenious alternative pathway for manipulating the adhesive performance. Notably, reducing the interfacial adhesion strength *via* the hydration of the functional groups in the adhesive at the substrate interface represents an ingenious strategy for achieving adhesive peelability. Accordingly, hot water immersion, as a low-cost, pollution-free, and facile stimulus method, enables selective peeling under mild conditions, outperforming the use of strong chemical solvents or high-energy radiation while minimizing substrate damage to the utmost extent.[25–28] However, for UV-curable acrylate adhesives, the realization of hot-water-assisted peelability remains a formidable challenge, which hinges on two critical trade-offs: balancing the cohesive strength and interfacial adhesion strength of the adhesive and reconciling the contradiction between high interfacial adhesion strength and efficient water penetration-induced hydration. Thus, precise manipulation of chemical structures and cross-linking networks to endow adhesives with ultrahigh interfacial adhesion strength, superior peelability, and recyclability has become a core research priority in this field.

To address the aforementioned issues, this study developed a cohesion-adhesion synergy-guided molecular engineering strategy to fabricate UV-curable adhesives with the integrated properties of superior bonding strength and hot water-triggered peelability. A custom-synthesized UV-curable difunctional polyurethane acrylate (PM1) with a tailored hard-soft segment structure was blended with a mixture of complementary acrylate monomers to construct a novel adhesive system. The soft segments in the PM1 molecular chain, which are derived from polytetrahydrofuran diol and polyester diol, endow the polymer with excellent molecular chain mobility, thereby laying a solid foundation for segment migration under hot-water conditions. Meanwhile, the carbamate moieties within the hard segments serve as physical cross-linking sites, which effectively boost the toughness and impact resistance of the material. Simultaneously, the polar groups in these segments strengthen the interfacial adhesion and substrate compatibility *via* robust van der Waals interactions and hydrogen bonding with diverse substrate surfaces. Furthermore, the incorporation and compositional optimization of polar acrylate monomers further regulate the cohesive energy of the adhesive system as well as its surface wettability and interfacial adhesion toward substrates, thereby achieving synergistic enhancement of both cohesive and adhesive properties. The structure-property relationships that govern the composition, bonding performance, mechanical properties, and hot-water peel efficiency of UV-curable adhesives were systematically investigated *via* a combination of experimental studies and molecular dynamics simulations. The as-prepared adhesive exhibited superior interfacial adhesion strength on diverse substrate surfaces, coupled with excellent peelability and reusability, thereby achieving an optimal balance between robust interfacial bonding strength and efficient peelability. This study proposes a versatile and scalable strategy for the rational design of high-performance functional adhesives, which not only provides novel structural design insights for hot water-peelable UV-acrylate adhesives, but also paves the way for advancing their practical application in electronic product recycling and sustainable manufacturing.

EXPERIMENTAL

Materials

Dicyclohexylmethane-4,4'-diisocyanate (HMDI), stannous octoate, and tetrahydrofurfuryl acrylate (THFA) were purchased from Shanghai Aladdin Biochemical Technology Co., Ltd. Tetrahydrofurfuryl acrylate (HEA), *N*,*N*-dimethylacrylamide (DMAA), isobornyl acrylate (IBOA), 2,2-dimethoxy-2-phenylacetophenone (651), and diphenyl (2,4,6-trimethylbenzoyl) phosphine oxide (TPO) were purchased from Shanghai Macklin Biochemical Co., Ltd. Polyester diol (S-1011-35) and polytetramethylene ether glycol (PTMG2000) were purchased from Badische Anilin-und-Soda-Fabrik. All other reagents were of analytical grade and were utilized as received without additional purification.

Synthesis of PM1

Briefly, PTMG (0.2 mol, 200 g) and S-1011-35 (0.1 mol, 100 g) were added into a 250 mL three-necked flask, followed by vacuum drying at 120 °C for 2 h to eliminate residual moisture. After cooling to 70 °C, HMDI (0.315 mol, 82.64 g) was added dropwise to the three-necked flask, followed by continuous stirring for 30 min. Subsequently, stannous octoate was added dropwise into the flask, and the temperature was increased sequentially to 90 °C and further to 100 °C with continuous stirring maintained for 2 h. After cooling to 90 °C, HEA (0.33 mol, 38.32 g) was added to conduct end-capping of the residual isocyanate groups, and the mixture was stirred for an additional 1 h, yielding the UV-curable resin (designated as PM1). Finally, the PM1 resin was cooled to 60 °C, followed by the addition of IBOA as the solvent, and the mixture was continuously stirred for 1 h to yield a PM1 resin/IBOA hybrid component with an IBOA mass fraction of 10.60 wt%.

Fabrication of UV-curable Adhesives

A 250 mL three-necked flask was charged with a mixture of PM1/IBOA (20–50 g), THFA (30 g), DMAA (0–20 g), photoinitiator 651 (2.5 g), and photoinitiator TPO (2 g). The resultant mixture was magnetically stirred at 25 °C for 3 h under a nitrogen atmosphere to ensure homogeneity and subsequently transferred to a brown vial for sealed storage. With the other components fixed, the naming convention of the adhesive formulations is defined as follows: taking "30-10"as an example, 30 denotes the content of PM1/IBOA (30 g), and 10 represents that of DMAA (10 g). The fabricated adhesive was exposed to a 365 nm ultraviolet mercury lamp (521.89 mW/cm^2) for 30 s to yield a UV-cured film.

https://doi.org/10.1007/s10118-026-3677-7

Characterizations

Fourier transform infrared (FTIR) spectra were recorded on a Nicolet Is10 FTIR spectrophotometer (Thermo Fisher, USA) in the range of 500–4000 cm^{-1}, using KBr as the substrate. ^{1}H-NMR spectra were obtained using an Advance III 400 MHz NMR spectrometer (Bruker, Germany) with deuterated chloroform ($CDCl_3$) as the solvent. The molecular weight and dispersity ($Đ$) of the samples were analyzed using a Waters 1500 gel permeation chromatography with THF as the solvent. Thermogravimetric analysis (TGA) was performed on a TGA 55 instrument, with temperatures ranging from 20 °C to 800 °C at a heating rate of 10 °C/min. Lap shear, tensile, and peel strength tests were performed on a CMT-4503 mechanical tensile testing machine (SUST, China) at crosshead speeds of 50, 300, and 300 mm/min, respectively (Refer to the Supporting Information for the detailed testing procedure). The surface morphology and elemental distribution of the samples were studied using a Zeiss Gemini 300 field-emission scanning electron microscope (SEM).

RESULTS AND DISCUSSION

Characterization of the Adhesive Structure and Properties

On-demand peelable UV-curable adhesives with superior bonding strength were formulated using custom-synthesized difunctional polyurethane acrylate (PM1) as the crosslinker and blended with complementary acrylate monomers (Fig. 1). As shown in Fig. 1(a), the novel PM1 resin was synthesized using polyester diol (S-1011-35), polytetrahydrofuran diol (PTMG2000), dicyclohexylmethane diisocyanate (HMDI), and 2-hydroxyethyl acrylate (HEA) as raw materials, with isobornyl acrylate (IBOA) as the reactive diluent. Under the catalytic influence of tin octoate, a nucleophilic addition reaction occurs between the —OH groups in the diols and the —NCO groups in HMDI, resulting in the formation of carbamate groups. The reaction terminates with monofunctional hydroxyethyl acrylate (HEA), which introduces double bonds as reactive sites for subsequent UV curing of the adhesive. Finally, the reactive UV monomer IBOA was incorporated as a solvent to reduce the viscosity of PM1, thereby facilitating the subsequent adjustment and optimization of the adhesive formulation (Fig. 1b). A UV-curable adhesive system was successfully fabricated by integrating the as-synthesized difunctional PM1 resin/IBOA hybrid component with *N*,*N*-dimethylacrylamide (DMAA) and tetrahydrofurfuryl acrylate (THFA) monomers. As illustrated in Fig. 1(c), upon UV curing, polyurethane acrylate (PM1) serves as a crosslinker to construct a robust yet flexible crosslinking network, which ensures excellent cohesive strength, whereas its soft segments derived from polytetrahydrofuran diol and polyester diol endow the network with superior molecular chain mobility. Additionally, the incorporation of polar acrylate monomers enables the construction of a network of non-covalent interactions (*e.g.*, hydrogen bonds) between molecular chains while simultaneously improving the surface wettability and substrate interfacial adhesion of the adhesive, thus achieving synergistic enhancement of its cohesive and adhesive properties.

The chemical structures of the as-synthesized PM1 and the corresponding monomer precursors were fully elucidated *via* FTIR and ^{1}H-NMR spectroscopy. As depicted in Fig. 2(A), the characteristic bands at 3417, 3471, and 3503 cm^{-1} are attributed to the O—H stretching vibrations of the hydroxyethyl acrylate (HEA), polytetrahydrofuran ether diol (PTMG2000), and polyester diol (S-1011-35), respectively. The bands at 2931 and 2871 cm^{-1} were assigned to the asymmetric and symmetric stretching vibrations of the methylene groups in both the as-synthesized PM1 and its corresponding monomer precursors, respectively. Meanwhile, the distinct band at 1733 cm^{-1} corresponds to the asymmetric stretching vibration of the ether linkage. The FTIR spectrum of bicyclohexylmethane diisocyanate (HMDI) exhibited a characteristic peak at 2243 cm^{-1} corresponding to the N=C=O group. In the spectrum of the as-synthesized PM1 resin, the peaks at 3329 and 1724 cm^{-1} indicate N—H stretching and C=O stretching, respectively. The disappearance of the isocyanate peak at 2243 cm^{-1} and the presence of the N—H stretching peak at 3329 cm^{-1} confirmed the successful synthesis of PM1.[29–31] ^{1}H-NMR spectroscopy was used to further verify the chemical structure of the as-prepared PM1 resin. As shown in Fig. 2(B), three distinct new peaks at 5.87, 6.19, and 6.46 ppm were observed, which confirmed the successful incorporation of double bonds into the chain structure of the PM1 resin. These results prove the successful synthesis of the PM1 resin. The molecular weight (M_n) and dispersity ($Đ$) of the as-synthesized PM1 resin were 1.23×10^4 g/mol and 1.60, respectively (Fig. S1 in the electronic supplementary information, ESI). Furthermore, TGA revealed that the PM1 resin underwent 5% weight loss ($T_{d5\%}$) at temperatures above 275 °C, demonstrating its excellent thermal stability (Fig. 2C).

The as-synthesized difunctional PM1, upon blending with complementary acrylate monomers and subsequent UV curing, yields the target adhesives. The photocuring kinetics, micro-mesostructures, thermal properties, and rheological behaviors of the resultant adhesives were systematically characterized and analyzed. The conversion rate of C=C double bonds was calculated from the FTIR spectra recorded at different curing times (Fig. S2 in ESI). The characteristic peak of the C=C double bonds at 808 cm^{-1} gradually diminished with prolonged curing time and nearly vanished completely at 10 s, demonstrating full curing of the copolymer. Furthermore, integration area calculations revealed that the C=C double bond conversion reached 98.75% after 8 s of UV irradiation and approaches100% at 10 s. As illustrated in Fig. S3 (in ESI), the precursor PTMG2000 displayed distinct crystalline diffraction peaks. In contrast, only a broad amorphous halo was detected for the corresponding cured adhesives. This phenomenon can be ascribed to the introduction of reactive diluents, which exert a "solvation-like effect" on PTMG2000 chains *via* intermolecular interactions (*e.g.*, van der Waals forces and hydrogen bonding), thus inhibiting the aggregation and ordered alignment of crystalline segments in PTMG2000 chains. Moreover, subsequent crosslinking anchors the PTMG2000 chains between adjacent crosslinking nodes, which further impedes the mobility and ordered arrangement of the molecular chains, ultimately leading to the predominance of the amorphous phase in the polymer.[32] Meanwhile, TGA analysis revealed that the $T_{d5\%}$ of all adhesive samples exceeded 220 °C, demonstrating their excellent thermal stability and broad temperature adaptability for practical applications (Figs. S4a and S4b in ESI). Furthermore, the

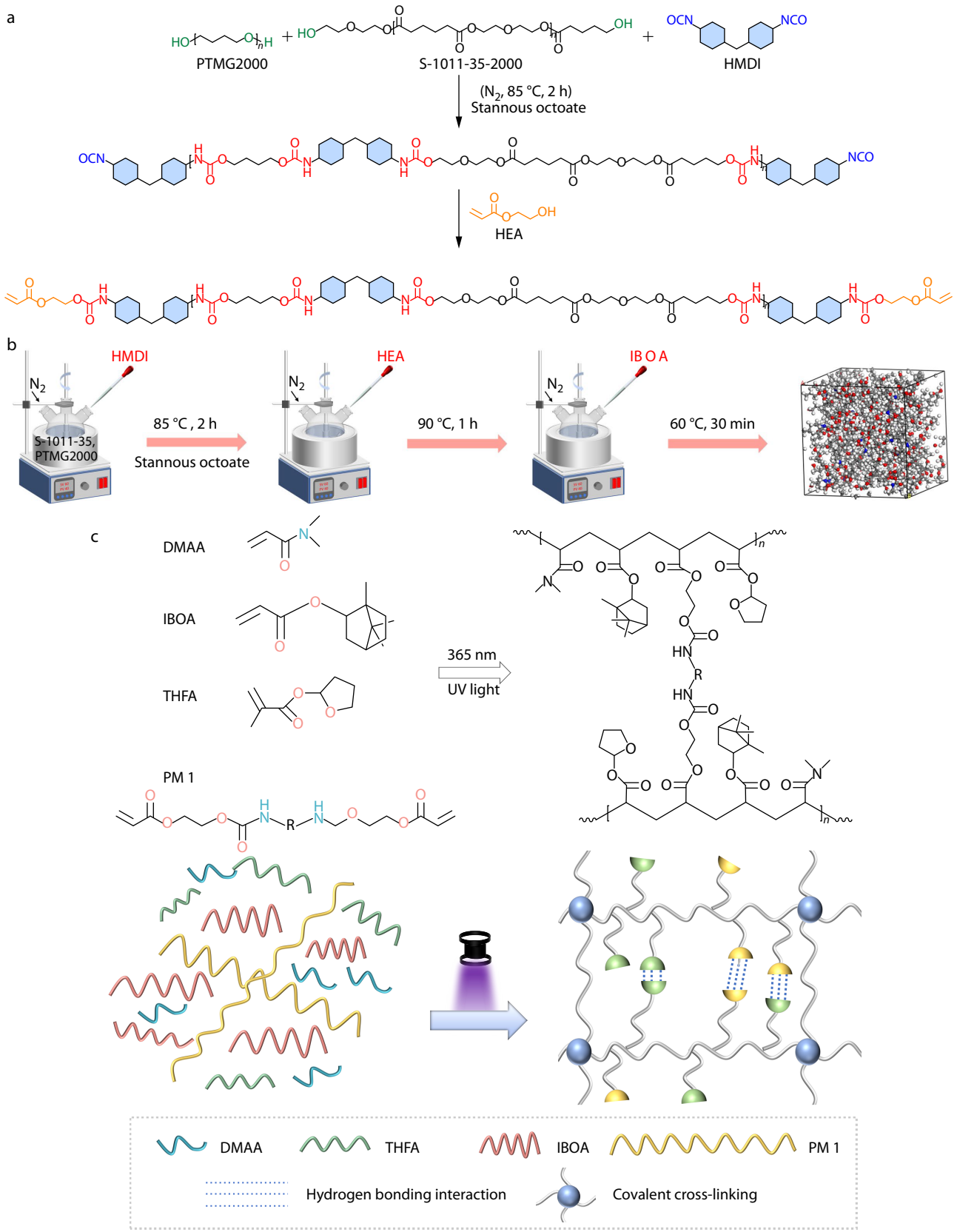

Fig. 1 Molecular structure (a) and synthetic route scheme (b) of the PM1 resin; (c) Schematic diagram of the curing mechanism and intermolecular chain interactions of the UV-curable adhesive.

https://doi.org/10.1007/s10118-026-3677-7

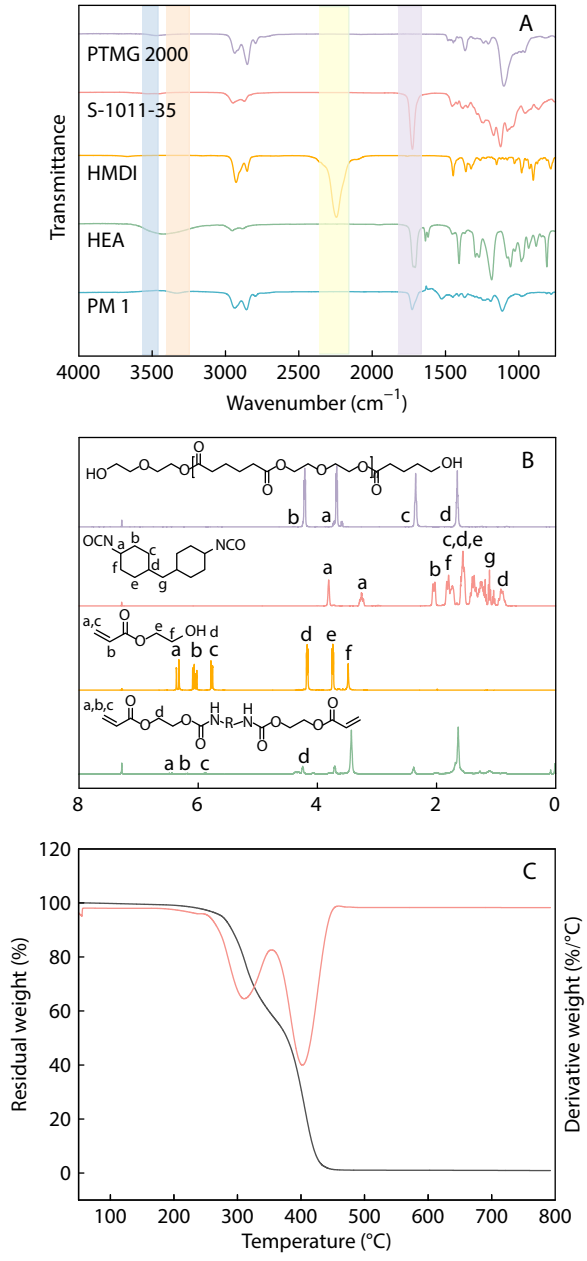

Fig. 2 (A) FTIR spectra and (B) ^{1}H-NMR spectra of the as-synthesized PM1 and its corresponding monomer precursors; (C) Thermogravimetric analysis (TGA) and derivative thermogravimetry (DTG) curves of PM1.

glass transition temperatures (T_g) of the adhesive films ranged from 18 °C to 41 °C, and their storage modulus remained substantially higher than the loss modulus over a broad temperature range, demonstrating that these adhesives can maintain their elastic state over a wide temperature range (Figs. S4c and S5 in ESI). A high loading of PM1 resin leads to a lower T_g of the adhesive, which is attributed to the high chain flexibility of the polyether diol or polyester diol soft segments in PM1. The incorporation of DMAA into the adhesive formulation leads to a remarkable elevation in the T_g of the adhesive, which is attributed to the strong polar amide groups (—CO—NH—) in DMAA, which substantially enhance intermolecular chain interactions and reduce free volume, thus impairing the mobility of molecular chains.[33,34] Moreover, the rheological properties of the adhesives were characterized *via* frequency and strain sweep rheological tests (Fig. S6 in ESI). Across the entire frequency range, the storage modulus of the adhesives remained consistently higher than the loss modulus, indicating the solid-like characteristics and excellent elastic behavior of all the adhesives under external stimuli. Upon the incorporation of DMAA, both the loss and storage moduli were enhanced, which can be ascribed to the strengthened non-covalent interactions between the molecular chains. In the strain sweep test, the storage modulus remained higher than the loss modulus at a strain amplitude of approximately 10%, demonstrating the structural integrity of the adhesive network and reversibility of the induced deformation. However, as the strain continued to increase, the adhesive films (*e.g.*, 30 and 50-10) featuring extremely low or high crosslinking density and intermolecular chain interactions transitioned from the linear viscoelastic region at small strains to the nonlinear region at large strains, accompanied by a concomitant decline in the storage modulus. This is primarily attributed to irreversible molecular chain slippage under large strains or destruction of the cross-linked microstructure induced by low molecular chain mobility and insufficient stress energy.[35,36] Notably, adhesive films (*e.g.*, 30-10) with a tailored molecular chain network structure exhibit high structural stability, where the molecular chains and crosslinking sites maintain elastic responses without fracture or irreversible flow even at relatively high strains (*e.g.*, ≥100%), which is consistent with their excellent combination of peelability and high interfacial adhesion, as elaborated subsequently (Fig. S6 in ESI).

Effect of PM1 Resin and DMAA Content on the Adhesive Properties

The bifunctional PM1 resin synthesized herein features a distinct soft-hard segment chain architecture, which plays a pivotal role in endowing the resultant adhesive with a tailored crosslinking network and excellent stress dissipation capability. To investigate the effect of PM1 resin content on adhesive properties, a fixed amount of THFA (30 g), photoinitiator 651 (2.5 g), and TPO (2 g) were incorporated into the adhesive formulation. The as-prepared PM1 resin exhibited a relatively high viscosity, which impaired the processability of the optimized adhesive formulation. As detailed in the **EXPERIMENTAL** section, PM1 resin was employed in the form of PM1/IBOA blends for the subsequent formulation design. The shear strength, stress-strain behavior, toughness, and peel strength of the adhesive were systematically evaluated as a function of the added content of the PM1/IBOA blends (Figs. 3a–3d). As shown in Fig. 3(a), the shear strength of the as-prepared adhesives ranges from 3.12 MPa to 3.81 MPa, which was dominated by intermolecular interactions between the functional groups of the adhesives and the substrate surface at the interface. However, at low loading levels of PM1 resin (*e.g.*, 10 and 20 g), the resultant adhesive exhibited low crosslinking density and cohesive energy, leading to cohesive failure with residual adhesive remaining on the substrate surface after peeling at room temperature (Table S1 in ESI). With the gradual increase in PM1 resin content, the tensile strength and elongation at break of the adhesive films in-

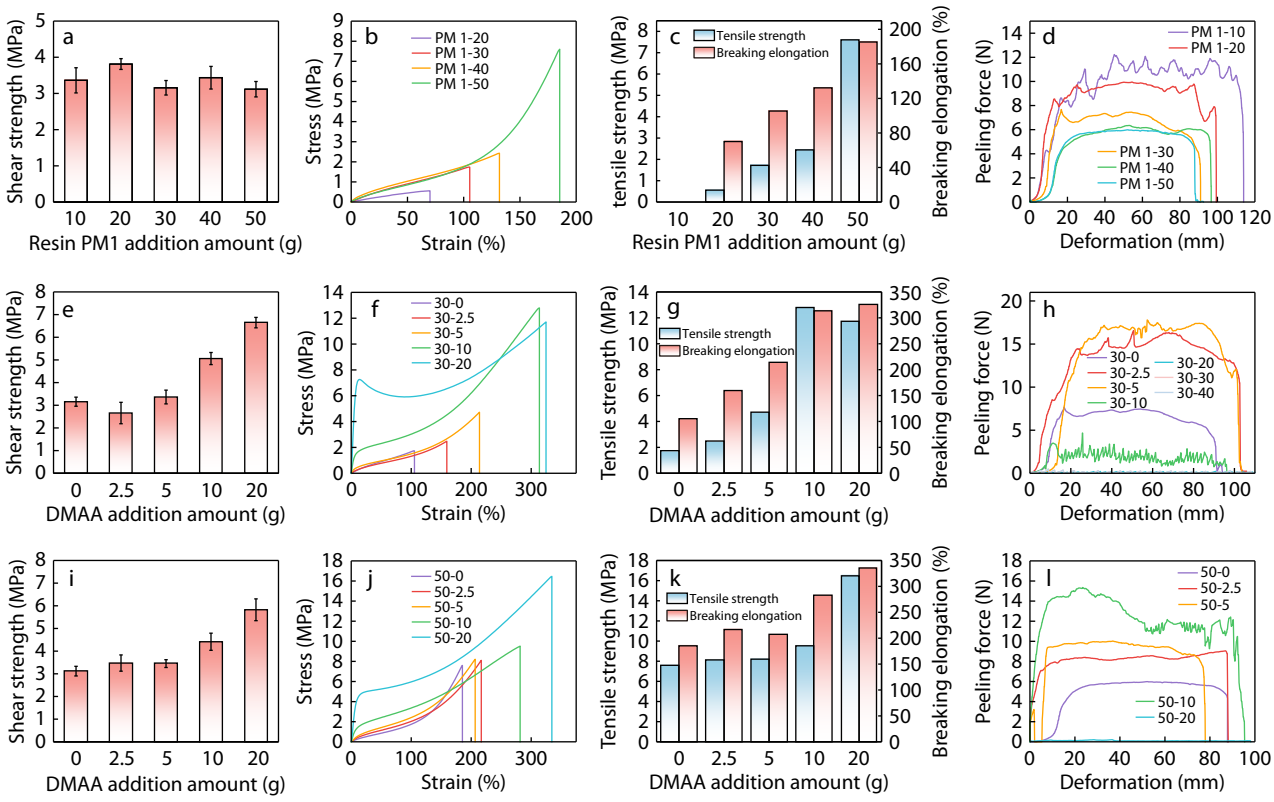

Fig. 3 Lap shear strength (a), stress-strain curves (b), tensile strength and breaking elongation (c), and peel curves at room temperature (d) of the adhesives with different PM1/IBOA content; Effect of DMAA content on the adhesives properties with PM1/IBOA content were fixed at 30 g (e–h) and 50 g (i–l): Lap shear strength (e, i), stress-strain curves (f, j), tensile strength and breaking elongation (g, k) and peel curves at room temperature (h, l).

creased sequentially to 7.60 MPa and 185.34%, respectively, which is attributed to the enhanced crosslinking density of the adhesive system and the improved toughness derived from the unique soft-hard segment structure of PM1 (Figs. 3b and 3c). Notably, the peel strength of the adhesives progressively decreased with increasing PM1 content (Fig. 3d). This is attributed to the absence of cohesive failure during peeling, which renders interfacial adhesion (*i.e.*, adhesive tackiness) the dominant determining factor. As previously noted, the high viscosity of PM1 compromises the wetting capacity of the adhesive on the substrate surface, thereby impairing the ultimate peel strength (Table S1 in ESI). The synergistic balance between cohesive energy and interfacial adhesion endows the adhesive with excellent peelability. Considering the integrated effects of PM1 on shear strength, stress-strain behavior, and peel strength, PM1-30 and PM1-50 were selected for further investigation to elucidate the impact of DMAA content on adhesive performance.

It is well established that the adhesion of adhesives to substrate surfaces proceeds *via* two pivotal steps: wetting and intermolecular force formation. Notably, adhesive viscosity plays a critical role in governing both the application processability and ultimate bonding performance. Accordingly, the incorporation of the polar reactive diluent DMAA into the adhesive formulation not only reduced the adhesive viscosity and enhanced the substrate wettability, but also simultaneously boosted the cohesive energy and interfacial bonding strength of the adhesive. To elucidate the effect of the DMAA content on adhesive performance, adhesive formulations were prepared with fixed loadings of PM1/IBOA (30 or 50 g), THFA (30 g), photoinitiator 651 (2.5 g), and TPO (2 g). As shown in Figs. 3(e)–3(m), the lap shear strength, tensile strength, elongation at break, and peel strength of the adhesive exhibited a consistent upward trend with increasing DMAA content. This performance enhancement stems from the incorporation of polar DMAA, which reinforces intermolecular chain interactions and interfacial bonding with the substrate while concurrently increasing the cohesive energy and interfacial adhesion energy of the adhesive system.[37–42] At a DMAA content of 10 g in the adhesive formulations, the resultant system achieved an optimal balance of mechanical properties, interfacial bonding strength, and peelability (Tables S2 and S3 in ESI). For the adhesive formulation with PM1/IBOA of 30 g (30-10), the shear strength, tensile strength, and elongation at break reached (5.06±0.27) MPa, 12.80 MPa and 313.70%, respectively. For the adhesive formulation with PM1/IBOA of 50 g (50-10), the shear strength, tensile strength, and elongation at break reached (4.41±0.38) MPa, 9.52 MPa and 281.53%, respectively. Additionally, the fatigue resistance of the as-prepared adhesives was characterized by subjecting 30-10 and 50-10 adhesive films to 20 loading-unloading cycles at a constant strain of 200% (Fig. S7 in ESI). A pronounced hysteresis appeared in the first cycle, which arose from the dissociation of the dynamic interchain hydrogen bonds within the adhesive elastomer. With further cycling, the hysteresis loop area decreased progressively and then plateaued, whereas the peak stress remained stable over mul-

tiple cycles, demonstrating excellent fatigue resistance, likely arising from a more uniform crosslinked network structure. Furthermore, the resultant adhesives (30-10 and 50-10) exhibited excellent peelability after immersion in hot water at 60 °C, with no adhesive residues remaining on the substrate surface. Ultimately, adhesive formulations designated as 30-10 and 50-10 were identified as the optimal candidates for subsequent bonding performance evaluations.

Peelable Performance of the Adhesives

To systematically characterize and evaluate the peelable performance of the as-prepared adhesives, systematic peel strength tests were conducted to assess their peelability under ambient temperature conditions and after hot water immersion treatment. As depicted in Fig. 4(a), the peel strength of the adhesive on the glass substrate exhibited a gradual decline with increasing PM1 content in the formulation during room-temperature peel tests; however, the substantial adhesive residues observed at PM1 dosages of 10 and 20 g failed to meet the strict requirements for industrial applications. Notably, after immersion in 60 °C hot water for 3 min, all adhesives exhibited a significant decrease in peel strength, demonstrating excellent peelability, with no adhesive residue remaining on the glass substrate surface (Table S1 in ESI). To further investigate the effect of the DMAA content on the peel performance of the adhesive, peel tests were conducted at room temperature with a fixed content of PM1/IBOA maintained at 30 g (Fig. 4b). The results showed that peel strength increased significantly with the incorporation of DMAA; however, the adhesive exhibited residue on the glass substrate. Specifically, cohesive failure occurred in the room-temperature peel test, and substantial adhesive residue was observed on the glass substrate when the DMAA content reached 10 g, whereas the adhesive became unpeelable under the same testing conditions as the DMAA content increased to 20 g (Table S2 in ESI). Meanwhile, when the DMAA content did not exceed 10 g, the adhesive exhibited a sharp decline in peel strength after a 3 min immersion in 60 °C hot water, thus achieving excellent peelability with no adhesive residue remaining on the glass substrate. This result further validates that

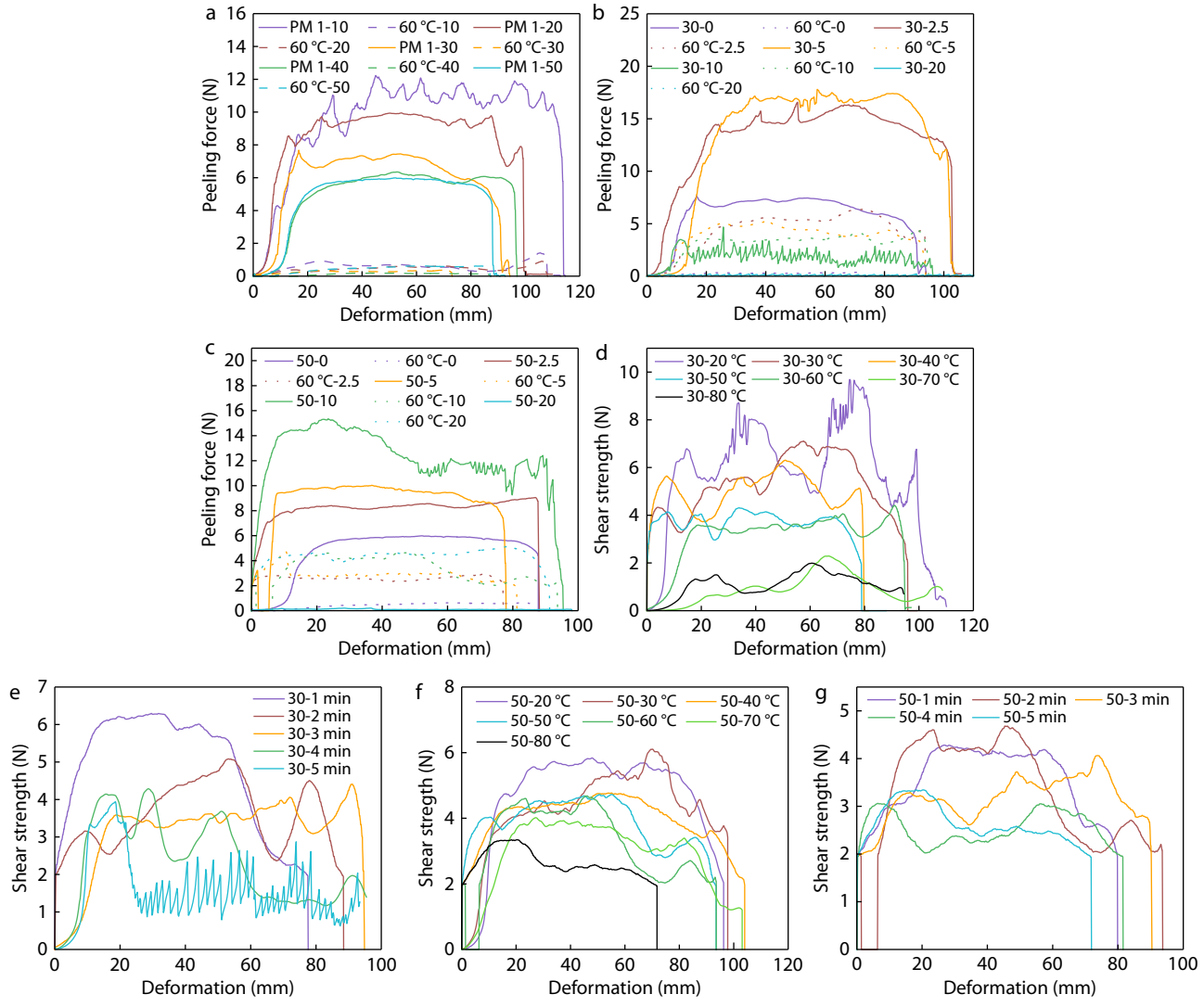

Fig. 4 Peeling curves of the adhesives with variable PM1/IBOA (a) and DMAA (b, c) content; Peeling curves of the adhesives (30-10 and 50-10) at different hot water soaking temperatures for 3 min (d, f) and different hot water soaking times at 60 °C (e, g).

https://doi.org/10.1007/s10118-026-3677-7

adhesive formulation 30-10 represents the optimal candidate, simultaneously endowed with exceptional peelability and robust interfacial adhesion to the substrate. When the PM1/IBOA content in the adhesive system was increased to 50 g, the crosslinking density of the cured adhesive network was significantly enhanced, thereby leading to a corresponding increase in the cohesive strength. As depicted in Fig. 4(c), with a gradual increase in DMAA content, the peel strength of the adhesive increased correspondingly; notably, the adhesive achieved an unpeelable state when the DMAA content reached 20 g (Table S3 in ESI). Similarly, the adhesive system (PM1/IBOA: 50 g) exhibited the optimal comprehensive performance in terms of mechanical strength, interfacial bonding strength, and hot-water immersion-assisted peelability when the DMAA content was 10 g. Adhesive formulations 30-10 and 50-10 were selected as model systems to further evaluate their peelable property under hot water immersion-assisted conditions (Figs. 4d–4g). As illustrated in Figs. 4(d) and 4(f), the peel strength of the adhesive decreases remarkably with an increase in the hot water immersion temperature, demonstrating excellent peelability. To guarantee residue-free detachment and satisfy the stringent demands of practical industrial applications, a hot-water immersion temperature of 60 °C was identified as the optimal processing condition. Furthermore, the effect of the hot water immersion duration on the peelability of the adhesive was systematically investigated. As depicted in Figs. 4(e) and 4(g), the peel strength of the adhesive decreased by as much as 60% after immersion in hot water at 60 °C for only 1 min. Consequently, the adhesive could be completely peeled off the glass substrate without any residual adhesive remaining (Fig. S8 in ESI). Notably, the peel strength of the adhesive gradually decreased with increasing impregnation time. Considering the requirements for sufficient peelability and operational efficiency, an impregnation duration of 3 min was selected as the optimal condition. The experimental results demonstrate that adhesive formulation 50-10 exhibits excellent peelability with no residual traces left, even after a short immersion of only 30 s in 20 °C warm water. This superior performance was attributed to the elevated loading of PM1, which effectively reinforced the cohesive strength of the adhesive matrix.[43,44] As a result, the adhesive enables reliable, residue-free peeling under synergistic conditions of low temperature and short immersion duration, thus satisfying the stringent application requirements of specific extreme operating environments.

Molecular Dynamics Simulation Analysis

It is well established that the interplay between adhesive strength and peelability represents an intrinsic trade-off in adhesive performance. To achieve robust adhesion while retaining satisfactory peelability, the precise modulation of the internal cohesiveness of the adhesive is of paramount importance. The peel force (F_{peel}) can be divided into vertical (F'_{peel}) and horizontal (F''_{peel}) components. The F'_{peel} is largely governed by the interfacial bonding strength between the adhesive and the substrate, whereas F''_{peel} is is predominantly correlated with the cohesive strength (*i.e.*, cohesive energy) of the adhesive.[45] For on-demand peelable adhesives, a moderate interfacial adhesion strength is required to satisfy practical application demands, whereas sufficient tensile strength and toughness must be ensured to avoid cohesive failure during the peeling process.

Taking adhesive 30-10 as a model system, molecular dynamics simulations were employed to investigate the cohesive energy density (CED) of the adhesive network and its interfacial interaction with the glass substrate (Figs. 5a–5f). Herein, the ball-and-stick molecular models of HMDI, PTMG2000, S-1011-35, HEA, DMAA, IBOA, and THFA were constructed and fully optimized using Materials Studio software. The polyurethane acrylate resin PM1 features a soft segment comprising 12 repeating units of PTMG2000 and four units of S-1011-35. A polymeric adhesive network was constructed *via* random copolymerization of the PM1 resin with the monomers DMAA, IBOA, and THFA. To construct the amorphous cell, a confined layer cell with a density of 1.0 g/cm^3 was adopted, coupled with the Compass III force field. Five molecular chains were included to calculate the cohesive energy of the polymer chains and their binding energy to the glass substrate, resulting in a ball-and-stick model with an approximate molecular weight of 6700. The model underwent geometric optimization through 25 annealing cycles, involving linear heating from 300 K to 800 K and cooling back to 300 K. The total simulation time under the NPT ensemble in one atmosphere was 40 ps (Figs. 5a–5c). Upon attaining a structurally optimized conformation, the CED of the polymer was calculated *via* the Forcite Cohesive Energy Density module, with the simulation parameters set to ultrafine quality and atomic charges assigned using the Compass III force field. To establish an interaction model between the adhesive network and glass substrate, the glass substrate was modeled as a pristine SiO_2 structure with the energy-minimized polymer model placed atop it. The system was first subjected to geometric optimization, followed by dynamic equilibration *via* the Forcite module, with all optimization parameters held constant throughout the process. The dynamic simulation was conducted at 333 K under the NVT ensemble for 40 ps, again using ultrafine quality settings and the Compass III force field. Figs. 5(a)–5(c) illustrate the interaction between adhesive 30-10 and the SiO_2 substrate over time, with the output results after 40 ps of dynamic simulation. The total energies of the system, network model, and glass model were computed *via* the Forcite Calculation Energy module, yielding an interaction energy of $E_{interaction} = E_{total} - (E_{surface} + E_{polymer}) = -452.133$ kcal/mol. Moreover, as shown in Figs. 5(d)–5(f), the cohesive energy densities for the adhesive without resin PM1, resin PM1, and adhesive 30-10 were calculated as 9.70×10^6, 1.11×10^8, and 2.29×10^8, respectively. Meanwhile, as depicted in Figs. 5(g)–5(j), hydrogen bonding interactions exist between the comonomer units and PM1 resin chain segments and among the PM1 resin chain segments in the adhesive system, as visualized *via* Materials Studio software (Table S4 in ESI). This result further confirms that the incorporation of the as-synthesized PM1 resin can significantly enhance the cohesive energy of the adhesive, thereby improving its peelability.

Adhesive Strength on Different Substrates

The as-prepared adhesive exhibited excellent cohesive strength and interfacial bonding strength, along with favorable peelability and recyclable bonding performance, outperforming previously reported adhesives (Fig. S9 in ESI).[46–53] As shown in Fig. 6(a), the adhesive was subjected to hot-water immersion-assist-

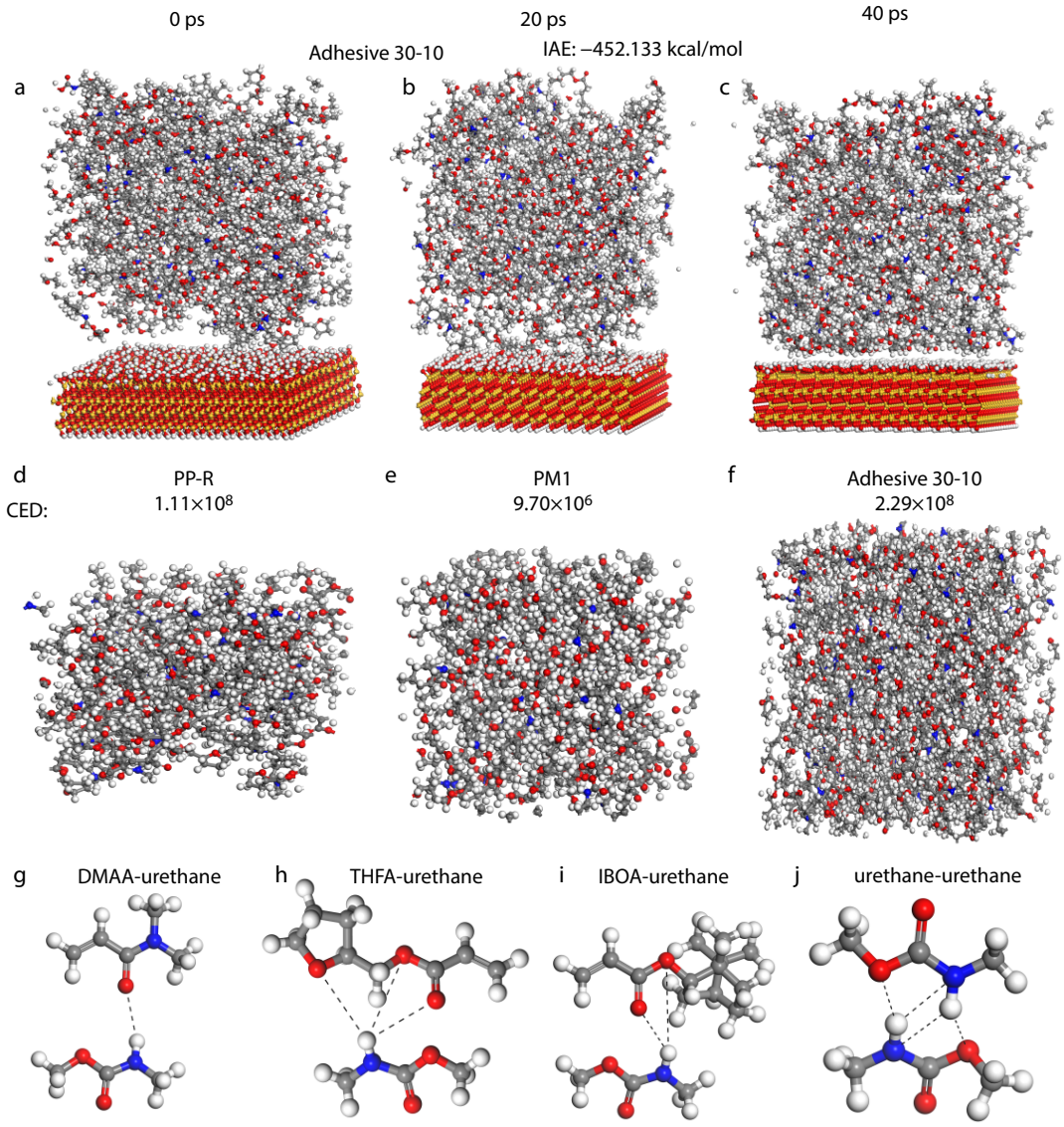

Fig. 5 Binding energy of the adhesive 30-10 with SiO_2 substrate at different time (a–c); Cohesive energy of the cured adhesives: witout resin PM1 (d), only resin PM1 (e), and adhesive 30-10 (f); Hydrogen bonding interactions between DMAA, THFA, IBOA, carbamate groups and carbamate groups (g–j).

ed peeling, followed by drying to remove residual water, and then thermally rebonded to the glass substrate for reuse. The rebonded adhesive exhibited excellent bonding strength, verifying its outstanding recyclability. Notably, the adhesive exhibited a certain degree of enhancement in bonding strength on the glass substrate surface after cyclic utilization under different heat treatment conditions compared with its initial UV-cured state. This phenomenon can be attributed to the fact that heat-induced treatment facilitates the rearrangement and optimization of the adhesive network structure, improves the wettability of the adhesive molecular chains on the substrate surface, and simultaneously mitigates the adverse effects of interfacial stress caused by UV curing shrinkage. Furthermore, the adhesive exhibited excellent bonding strength on the surfaces of various substrates, including poly(ethylene terephthalate) (PET), poly(methyl methacrylate) (PMMA), glass, steel, aluminum (Al), and epoxy-based composite plates (FR4). As shown in Fig. 6(b), the shear strengths of adhesive 30-10 on PMMA, glass, steel, Al, and FR4 are 8.49, 5.06, 3.10, 3.92, and 4.07 MPa, respectively. Notably, adhesive 30-10 exhibits excessively high bonding strength on the PET surface, which resulted in substrate fracture during the test. Similarly, the shear strengths of adhesive 50-10 on PET, PMMA, glass, steel, Al, and FR4 were 6.66, 4.41, 4.42, 2.15, 1.56, and 3.61 MPa, respectively. Interestingly, adhesive 30-10 exhibited a remarkable load-bearing capacity of over 20 kg when bonded to a glass substrate with a bonding area of 25 mm × 2 mm (Fig. 6c). Furthermore, cross-sectional SEM images and the corresponding SEM-EDS elemental mappings of the 30-10 adhesive film revealed the absence of bubbles and other defects within the film, along with a homogeneous distribution of C, N, and O elements across the cross-section (Fig. 6d). These results demonstrate excellent compatibility among the various components of the adhesive as well as superior film-forming performance.

https://doi.org/10.1007/s10118-026-3677-7

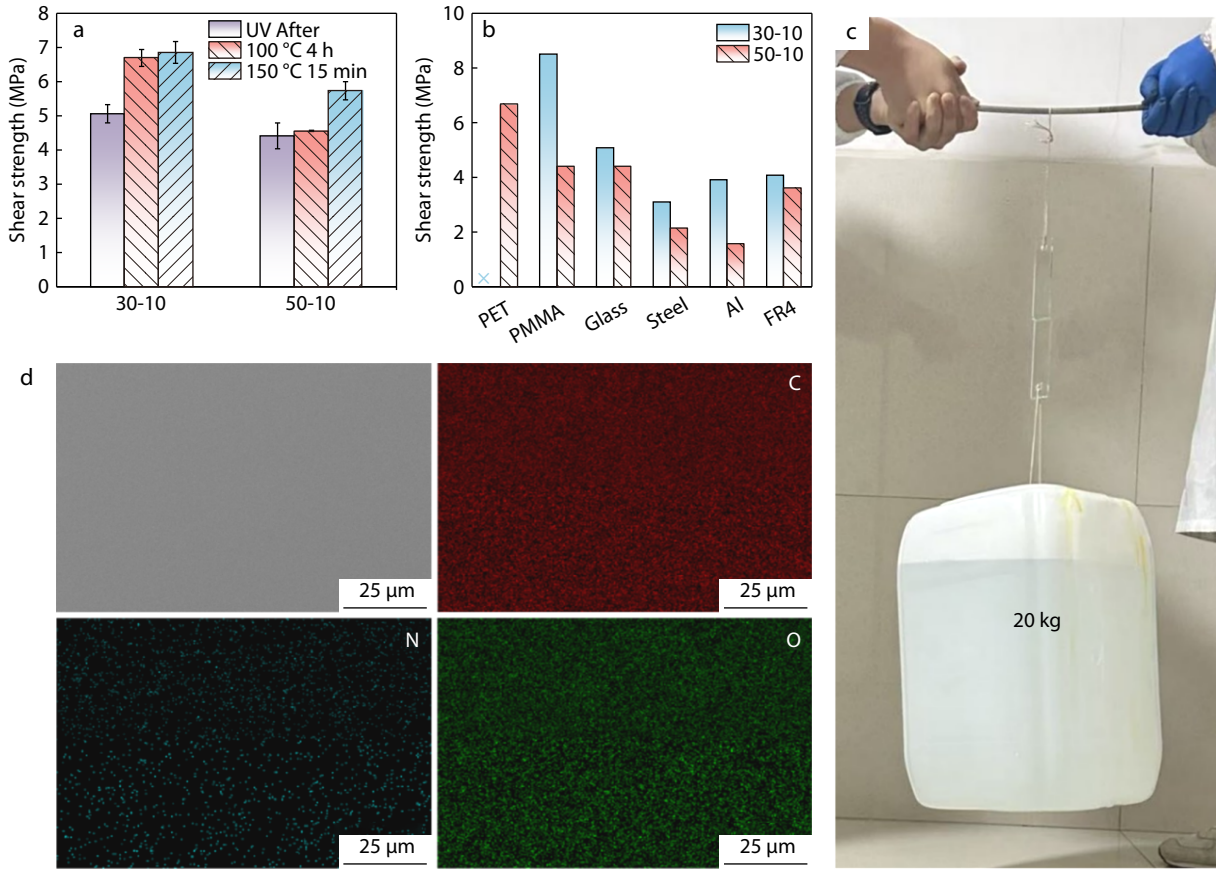

Fig. 6 (a) Shear strength of 30-10 and 50-10 adhesives on glass substrates under diverse treatment conditions: as-cured state, and hot water-assisted peeling followed by re-bonding *via* hot pressing at different temperatures after drying; (b) Shear strength of 30-10 and 50-10 adhesives on different substrates; (c) Real photograph of adhesive 30-10 with a load of 20 kg; (d) Cross-sectional SEM images and the corresponding SEM-EDS mappings of the adhesive 30-10 film.

CONCLUSIONS

In summary, on-demand peelable UV-curable adhesives with excellent bonding strengths were successfully fabricated *via* rational molecular engineering of cohesion-adhesion synergy. The peelable adhesive formulation was composed of custom-synthesized difunctional polyurethane acrylate and the corresponding complementary acrylate monomers. The difunctional polyurethane acrylate forms a robust, adaptable cross-linked network with high cohesive strength, and its soft segments endow the network with excellent molecular chain mobility and efficient stress dissipation. Furthermore, optimizing polar acrylate monomers precisely tailors the cohesive energy, surface properties, and interfacial adhesion of the system, achieving a synergistic enhancement in both cohesion and adhesion. The optimized adhesive achieved high shear strength (>5 MPa on glass substrates) and excellent peelability, enabling residue-free debonding within 3 min of immersion in water at 60 °C. The as-prepared adhesive exhibited excellent recyclable bonding performance, along with outstanding adhesive properties on the surfaces of various substrates. By rationally designing polymer architectures, this study presents a facile fabrication strategy for high-strength peelable adhesives and provides novel mechanistic insights, thereby advancing the recycling of electronics and sustainable manufacturing.

Conflict of Interests

The authors declare no interest conflict.

Electronic Supplementary Information

Electronic supplementary information (ESI) is available free of charge in the online version of this article at http://doi.org/10.1007/s10118-026-3677-7.

Data Availability Statement

The data supporting the findings of this study are available from the corresponding author upon reasonable request.

ACKNOWLEDGMENTS

This work was financially supported by the Natural Science Foundation of Shandong Province (Nos. ZR2022MB034 and ZR2025QC512), Key Research and Development Program of Shandong Province (No. 2024TSGC0909) and the National Natural Science Foundation of China (No. 52503154).

REFERENCES

1 Ito, S.; Akiyama, H.; Mori, M.; Yoshida, M.; Kihara, H. Azobenzene-containing triblock copolymer adhesive based on light-induced solid-liquid phase transition: application to bonding for various substrates. *Macromol. Chem. Phys.* **2019**, *220*, 1900105.

2 Mulcahy, K. R.; Kilpatrick, A. F. R.; Harper, G. D. J.; Walton, A.; Abbott, A. P. Debondable adhesives and their use in recycling. *Green Chem.* **2022**, *24*, 36–61.

3 Stamp, C. H.; Stumpp, J.; Calvino, C. Adhesives with debonding-on-demand capability: leveraging responsive microcapsules for mechanically-induced debonding. *Adv. Mater.* **2025**, *37*, 2414308.

4 Zhang, S. J.; Chen, X. X.; Cui, C. H.; Ma, L.; Zhong, Q. Y.; Shen, K. X.; Yu, J.; Li, Z.; Wu, Y. S.; Zhang, Q.; Cheng, Y. L.; He, L.; Zhang, Y. F. Strong, removable, and photoluminescent hyperbranched polyamide-amine hot melt adhesive. *Chinese J. Polym. Sci.* **2021**, *39*, 1319–1327.

5 Zheng, K.; Wang, J.; Chen, J.; Hao, J.; Liu, Z.; Xing, S.; Yang, J.; Chen, D. High-strength and debondable UV-curable adhesive based on dual-dynamic network. *Polym. Degrad. Stabil.* **2025**, *242*, 111665.

6 Robertson, F.; Wang, Y.; Rosing, H. An oligomeric switch that rapidly decreases the peel strength of a pressure-sensitive adhesive. *Int. J. Adhes. Adhes.* **2014**, *55*, 64–68.

7 Atif, M.; Ali, B.; Ramzan, I.; Younas, A.; Imran, M.; Ahmed, M. H.; Dilawaiz thermally stimulated bio-acrylate based detachable adhesives with sustainable bonding-debonding design. *Int. J. Adhes. Adhes.* **2025**, *136*, 103853.

8 Knight, S. J.; McCoy, J. D.; Chowdhury, S.; Lee, Y. Debonding-on-demand reversible adhesives via heat or light with competitive adhesion strength to conventional epoxy adhesives. *Polym. Test.* **2025**, *146*, 108776.

9 Liu, L.; Liu, Z.; Ren, Y.; Zou, X.; Peng, W.; Li, W.; Wu, Y.; Zheng, S.; Wang, X.; Yan, F. A superstrong and reversible ionic crystal-based adhesive inspired by ice adhesion. *Angew. Chem. Int. Ed.* **2021**, *60*, 8948–8959.

10 Ou, R.; Wang, S.; Li, J.; Li, Z.; Yu, L.; Wang, Z.; Murto, P.; Xu, X. Robust, switchable and printable underwater adhesives based on a temperature-deactivated design. *Adv. Funct. Mater.* **2024**, *35*, 2416043.

11 Skandalis, A.; Ayer, M. A.; Weder, C. Bioinspired adhesives with debonding-on-demand capability. *ACS Macro Lett.* **2025**, *14*, 420–427.

12 Wu, M.; Liu, Y.; Du, P.; Wang, X.; Yang, B. Polyurethane hot melt adhesive based on diels-alder reaction. *Int. J. Adhes. Adhes.* **2020**, *100*, 102597.

13 Zhang, H.; Guo, M. Thermoresponsive on-demand adhesion and detachment of a polyurethane-urea bioadhesive. *ACS Appl. Mater. Interfaces* **2024**, *16*, 43180–43188.

14 Kim, D.; Kim, H.; Jeon, W.; Kim, H. J.; Choi, J.; Kim, Y.; Kwon, M. S. Ultraviolet light debondable optically clear adhesives for flexible displays through efficient visible-light curing. *Adv. Mater.* **2024**, *36*, 2309891.

15 Lin, Z.; Feng, J.; Fang, L.; Zhang, Y.; Ran, Q.; Zhu, Q.; Yu, D. Transforming commercial polymers into tough yet switchable

Graphical Abstract

On-demand Peelable UV-curable Adhesives with Superior Bonding Strength: Rational Molecular Engineering of Cohesion-Adhesion Synergy

Wen-Qian Liu, Peng Wang, Hao-Kai Yuan, Lin Zhang, Bin Chen, Hong-Fei Jiang, Yi-Ran Wang, Lu Wang, Shu-Sheng Li, and Chuan-Yong Zong

University of Jinan; Shandong Institute of Non-Metallic Materials; Tianjin University

This study reports on-demand peelable UV-curable adhesives with outstanding bonding strength, hot-water-triggered debonding, and recyclable adhesion, which show great promise for electronic device recycling and sustainable manufacturing.

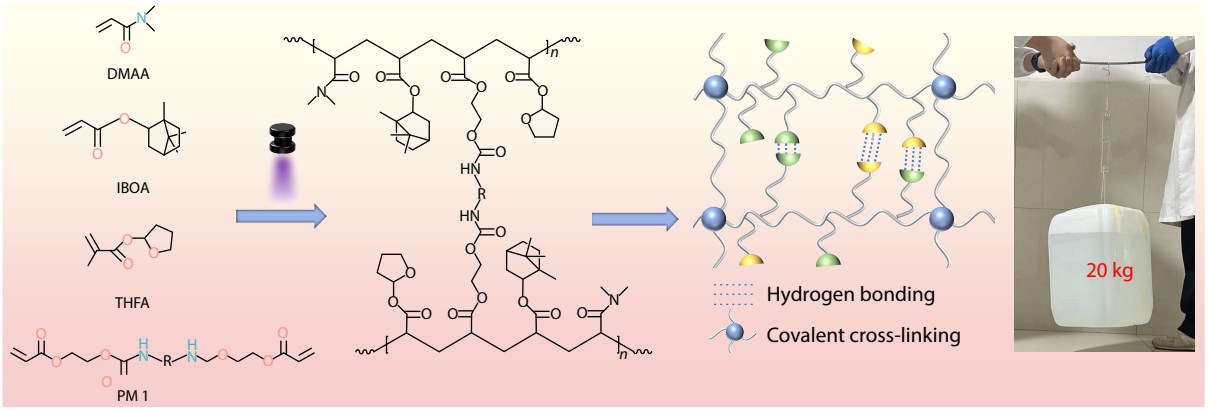

Chinese J. Polym. Sci. 2026, 44, 3053–3065 *https://doi.org/10.1007/s10118-026-3677-7*

adhesives by trident photoswitch molecule doping: break adhesion-switchability paradox. *Adv. Mater.* **2024**, *36*, 2406459.
16 Oh, X. Y.; Thi, Q. V.; Yu, M. M. L.; Izadyar, M.; Abedi, S. A. A.; Liu, X.; Truong, V. X. Moisture tolerance, thermally stable and light switchable adhesives platform based on reversible redshifted [2 + 2] photocycloaddition. *Adv. Funct. Mater.* **2025**, *35*, 2421823.
17 Wang, G.; Huang, X.; Zhou, Z.; Zhang, Y.; Yu, Y. Enabling (De)bonding on-demand with optically switchable pressure sensitive adhesive tape via photodimerization. *Chem. Eng. J.* **2024**, *499*, 155820.
18 Salimi, S.; Babra, T. S.; Dines, G. S.; Baskerville, S. W.; Hayes, W.; Greenland, B. W. Composite polyurethane adhesives that debond-on-demand by hysteresis heating in an oscillating magnetic field. *Eur. Polym. J.* **2019**, *121*, 109264.
19 Zhang, Z.; He, R.; Han, B.; Ren, S.; Fan, J.; Wang, H.; Zhang, Y. L.; Ma, Z. C. Magnetically switchable adhesive millirobots for universal manipulation in both air and water. *Adv. Mater.* **2025**, *37*, 2420045.
20 Zhao, J.; Li, X.; Tan, Y.; Liu, X.; Lu, T.; Shi, M. Smart adhesives via magnetic actuation. *Adv. Mater.* **2022**, *34*, 2107748.
21 Zhao, J.; Lu, T.; Zhang, Y.; Zhang, C.; Pan, C.; Tan, Y.; Zhu, J.; Li, B.; Zhang, L.; Shi, M.; Li, X. Magnetically actuated adhesives with switchable adhesion. *Adv. Funct. Mater.* **2023**, *33*, 2305484.
22 Sun, S.; Liu, J.; Yue, Q.; Lv, J.; Wang, S.; Wei, Y. Charge delocalization for electrically detachable poly(ionic liquids) ionoadhesives with ultrahigh mechanical robustness. *Macromolecules* **2024**, *57*, 9355–9366.
23 Walter, K.; Hoch, D. P.; Hertweck, L.; Balasubramanian, K.; Geisler, J.; Röllig, M.; Neubert, T. J.; Börner, H. G. Unlocking the Essence of Lignin: High-performance adhesives that bond via thiol-catechol connectivities and debond on electrochemical command. *Adv. Mater.* **2025**, *37*, e10463.
24 Wei, Y.; Wu, M.; Sun, S.; Liu, J.; Yue, Q.; Chen, Y. Electrically detachable ionic conductive epoxy adhesives with high bonding strength. *ACS Appl. Polym. Mater.* **2023**, *5*, 7328–7339.
25 Ju, Y. H.; Lee, H. J.; Han, C. J.; Lee, C. R.; Kim, Y.; Kim, J. W. Pressure-sensitive adhesive with controllable adhesion for fabrication of ultrathin soft devices. *ACS Appl. Mater. Interfaces* **2020**, *12*, 40794-40801.
26 Mehravar, E.; Gross, M. A.; Leal, G. P.; Reck, B.; Leiza, J. R.; Asua, J. M. Phase separation driven on-demand debondable waterborne pressure-sensitive adhesives. *Polymers* **2018**, *10*, 975.
27 Wan, Y.; Huang, S.; Sun, Y.; Zhu, H.; Zheng, Q.; Zhang, Q.; Zhu, S. Superstrong yet water-detachable eutectogel adhesives. *Chem. Eng. J.* **2022**, *442*, 136289.
28 Ma, Y.; Jiang, X.; Shi, Z.; Berrocal, J. A.; Weder, C. Closed-loop recycling of vinylogous urethane vitrimers. *Angew. Chem. Int. Ed.* **2023**, *62*, e202306188.
29 Ding, H.; Liu, L.; Wang, C.; Sun, N.; Wu, L.; Lin, B.; Zhou, K.; Zhang, W.; Qian, X.; Shi, C.; Yu, B. Highly transparent, mechanically strong, recyclable, and flame-retardant vanillin-modified poly(urethane-urea) elastomers via dynamic oxime-urethane bonds and hydrogen bonds. *Chem. Eng. J.* **2025**, *514*, 163416.
30 Huang, R.; Zhao, F.; Li, Y.; Jiang, Z.; He, F.; Zhang, K.; Chen, Z.; He, G.; Yang, W. GO-enhanced polyurethane phase change materials with triple dynamic bonds: Oxime-urethane, coordination and hydrogen bonds. *Chem. Eng. J.* **2025**, *522*, 168010.
31 Wu, W.; Xuan, C.; Jiang, Y.; Lu, H.; Yan, S.; Shi, X. Polyurethane-based bioglue for the repair of arterial ruptures. *Adv. Funct. Mater.* **2024**, *35*, 2417402.
32 Wang X, Yang Z, Zhang Y, et al. Syncretic of soft, hard, and rigid segments cultivate high-performance elastomer. *Chem. Eng. J.* **2024**, *495*, 153466.
33 Bai, C.; Huang, X.; Xie, F.; Xiong, X. Microcrystalline cellulose surface-modified with acrylamide for reinforcement of hydrogels. *ACS Sustain. Chem. Eng.* **2018**, *6*, 12320–12327.
34 Zhu, Z.; Yang, Y.; Ding, G.; Lin, X.; Huang, L.; Li, J.; Chen, L. Advancing regenerated leather from waste leather fibers: robustness and thermal/water comfort. *Compos. Part A* **2026**, *203*, 109566.
35 Gibaud. T.; Dagès. N.; Lidon, P. et al. Rheoacoustic gels: tuning mechanical and flow properties of colloidal gels with ultrasonic vibrations. *Phys. Rev. X* **2020**, *10*, 011028.
36 Feng, S.; Xing, J. J.; Guo, X. N. Nonlinear rheological properties of chinese cold skin noodle (liangpi) and wheat starch gels by large amplitude oscillatory shear (laos). *Food Hydrocoll.* **2023**, *134*, 108030.
37 Zhao, C.; Zheng, H.; Gao, B.; Liu, Y.; Zhai, J.; Zhang, S.; Xu, B. Ultrasound-initiated synthesis of cationic polyacrylamide for oily wastewater treatment: enhanced interaction between the flocculant and contaminants. *Ultrason. Sonochem.* **2018**, *42*, 31–41.
38 Zeng, M.; Feng, Z.; Huang, Y.; Liu, J.; Ren, J.; Xu, Q.; Fan, L. Chemical structure and remarkably enhanced mechanical properties of chitosan-graft-poly(acrylic acid)/polyacrylamide double-network hydrogels. *Polym. Bull.* **2016**, *74*, 55–74.
39 Liu, Y.; Tian, B.; Liu, X. Effect of interaction enhancement on rheological response of polypropylene/polybutadiene blend composites. *Polym. Test.* **2021**, *96*, 107069.
40 Nan, L.; Liu, J.; Liu, C.; Quan, P.; Guo, J.; Fang, L. Fe(III)-coordinated N-[tris(hydroxymethyl)methyl]acrylamide-modified acrylic pressure-sensitive adhesives with enhanced adhesion and cohesion for efficient transdermal application. *Acta Biomater.* **2022**, *152*, 186–196.
41 Gong, K.; Sun, P.; Cai, Y.; Wang, X.; Pang, Y.; Liu, C.; Guo, J.; Fang, L. Water-compatible cross-linked pyrrolidone acrylate pressure-sensitive adhesives with persistent adhesion for transdermal delivery: synergistic effect of hydrogen bonding and electrostatic force. *Acta Biomater.* **2024**, *179*, 130–148.
42 Tiu, B. D. B.; Delparastan, P.; Ney, M. R.; Gerst, M.; Messersmith, P. B. Enhanced adhesion and cohesion of bioinspired dry/wet pressure-sensitive adhesives. *ACS Appl. Mater. Interfaces* **2019**, *11*, 28296–28306.
43 Kang, S.; Li, T.; Jiang, H.; Fu, Z.; Gao, R.; Chen, Q.; Xia, J. Optically clear pressure sensitive adhesives with multiple hydrogen bond cross-linking. *J. Polym. Res.* **2025**, *32*, 104.
44 Han, Y.; Gong, Z.; Zhou, R.; Li, W.; Shi, J.; Hu, J. Enhanced adhesion to low-surface-energy substrates using polyurethane acrylate/polyacrylate interpenetrating network pressure-sensitive adhesives. *Prog. Org. Coat.* **2025**, *206*, 109376.
45 Zhang, Z.; Zhang, B.; Zhang, Z.; Xie, Q.; Zhang, G.; Zhang, G.; Ma, C. Self-reinforcing gradient antifouling coating with high adhesion, on-demand peelability, and superior recyclability. *Adv. Funct. Mater.* **2025**, *35*, 2508400.
46 Hyder, M. J.; Godleman, J.; Chippindale, A. M.; Hallett, J. E.; Zinn, T.; Harries, J. L.; Hayes, W. Thermally and base-triggered "debond-on-demand" chain-extended polyurethane adhesives. *Macromolecules* **2025**, *58*, 681–696.
47 Ito, S.; Yamashita, A.; Akiyama, H.; Kihara, H.; Yoshida, M. Azobenzene-based (meth)acrylates: controlled radical polymerization, photoresponsive solid-liquid phase transition behavior, and application to reworkable adhesives. *Macromolecules* **2018**, *51*, 3243–3253.
48 Liu, Z.; Ren, X.; Zheng, H.; Xie, J.; Zhang, Q. Detachable, Self-repairing, and closed-loop recyclable self-initiated light-curing adhesives with controllable bonding strength. *ACS Appl. Mater. Interfaces* **2025**, *17*, 70276–70285.
49 Matsumura, Y.; Yamaoka, K.; Ikura, R.; Takashima, Y. Light stimuli-responsive degradable and tough polymeric materials with movable cross-links. *ACS Appl. Mater. Interfaces* **2025**, *17*,

20261−20269.
50 Ou, X.; Zou, X.; Liu, Q.; Li, L.; Li, S.; Cui, Y.; Zhou, Y.; Yan, F. Recyclable, fire-resistant, superstrong, and reversible ionic polyurea-based adhesives. *Chem. Mater.* **2023**, *35*, 1218−1228.
51 Umehara, M.; Miyazaki, I.; Suzumura, A.; Moribe, S.; Masuoka, Y. Dismantlable adhesive using coordination polymer/metal organic framework. *Sci. Rep.* **2025**, *15*, 38405.
52 Wang, C.; Li, P.; Zhang, S.; Zhang, G.; Tan, S.; Wu, Y.; Watanabe, M. Azobenzene molecular trigger controlling phase transitions of pnipam in ionic liquids and light-controlled adhesiveness. *Macromolecules* **2020**, *53*, 4901−4907.
53 Yue, Q.; Lv, J.; Huang, S.; Guo, Y.; Wang, Y.; Liu, J.; Sun, S.; Wang, M.; Wang, S.; Wei, Y. Electrically detachable and fully recyclable pressure sensitive ionoadhesive tapes. *Adv. Funct. Mater.* **2025**, *35*, 2423865.